Valve type, size and deployment location affect hemodynamics in an in vitro valve-in-valve model

Prem A. Midha, MS[a], Vrishank Raghav, PhD[a], Jose F. Condado, MD, MS[b], Ikechukwu Okafor, PhD[a], Stamatios Lerakis, MD[b], Vinod H. Thourani, MD[b], Vasilis Babaliaros, MD[b], Ajit P. Yoganathan, PhD[a,*]

[a]*Georgia Institute of Technology, Atlanta, GA*
[b]*Emory University Hospitals, Atlanta, GA*

Abstract

Objectives To optimize hemodynamic performance of valve-in-valve (VIV) according to transcatheter heart valve (THV) type (balloon vs. self-expandable), size and deployment positions in an in vitro model.
Background VIV transcatheter aortic valve replacement (VIV-TAVR) is increasingly used for the treatment of patients with a failing surgical bioprosthesis. However, there is a paucity in understanding the THV hemodynamic performance in this setting.
Methods VIV-TAVR was simulated in a physiological left heart simulator by deploying a 23mm SAPIEN, 23mm CoreValve, and 26mm CoreValve within a 23mm Edwards PERIMOUNT surgical bioprosthesis. Each THV was deployed into 5 different positions: normal (inflow of THV was juxtaposed with inflow of surgical bioprosthesis), -3mm and -6mm sub-annular, and +3mm and +6mm supra-annular. At a heart rate of 70 bpm and cardiac output of 5.0 L/min, mean transvalvular pressure gradients (TVPG), regurgitant fraction (RF), effective orifice area (EOA), pinwheeling index (PI), and pullout forces were evaluated and compared between THVs.
Results Though all THV deployments resulted in hemodynamics that would have been consistent with VARC-2 procedure success, we found significant differences between THV type, size, and deployment position. For a SAPIEN valve, hemodynamic performance improved with a supra-annular deployment, with the best performance observed at +6mm. Compared to a normal position, +6mm resulted in lower TVPG (9.31±0.22 mmHg vs. 11.66±0.22 mmHg; $p<0.01$), RF (0.95±0.60% vs. 1.27±0.66%; $p<0.01$), and PI (1.23±0.22% vs. 3.46±0.18%; $p<0.01$), and higher EOA (1.51±0.08 cm^2 vs. 1.35±0.02 cm^2; $p<0.01$) at the cost of lower pullout forces (5.54±0.20 N vs. 7.09±0.49 N; $p<0.01$). For both CoreValve sizes, optimal deployment was observed at the normal position. The 26mm CoreValve, when compared to the 23mm CoreValve and 23mm SAPIEN, had lower TVPG (7.76±0.14 mmHg vs. 10.27±0.18 mmHg vs. 9.31±0.22 mmHg; $p<0.01$) and higher EOA (1.66±0.05 cm^2 vs. 1.44±0.05 cm^2 vs. 1.51±0.08 cm^2; $p<0.01$), RF (4.79±0.67% vs. 1.98±0.36% vs. 0.95±1.68%; $p<0.01$), PI (29.13±0.22% vs. 6.57±0.14% vs. 1.23±0.22%; $p<0.01$), and pullout forces (10.65±0.66 N vs. 5.35±0.18 N vs. 5.54±0.20 N; $p<0.01$).
Conclusions The optimal deployment location for VIV in a 23 PERIMOUNT surgical bioprosthesis was at a +6mm supra-annular position for a 23mm SAPIEN valve and at the normal position for both the 23mm and 26mm CoreValves. The 26mm CoreValve had lower gradients, but higher RF and PI than the 23mm CoreValve and the 23mm SAPIEN. In their optimal positions, all valves resulted in hemodynamics consistent with the definitions of VARC-2 procedural success. Long-term studies are needed to understand the clinical impact of these hemodynamic performance differences in patients who undergo VIV-TAVR.

Keywords: Valve-in-valve, transcatheter aortic valve replacement, VIV, TAVR

1. Introduction

Valve-in-valve transcatheter aortic valve replacement (VIV-TAVR) has emerged as a treatment for high surgical risk patients with failing aortic surgical bioprostheses (1, 2). Recently, the Food and Drug Administration has approved both balloon-expandable (SAPIEN XT, Edwards Lifesciences, Irvine, CA, USA) and self-expanding (CoreValve, Medtronic, Dublin, Ireland) transcatheter heart valves (THV) for this indication in the US. While VIV-TAVR may restore valve function and improve symptoms, adverse events such as elevated post-procedural gradients (28.4%), coronary obstruction (3.5%), device malpositioning (15.0%) and valve leaflet thrombosis (4%) have been reported (3, 4, 5, 6). A lack of understanding of how VIV deployment location affects THV hemodynamics may explain some of these untoward events.

Current sizing and deployment recommendations are based on reference guides that use valve true internal diameters for THV size selection. As a consequence, commonly used guides, such as the ViV Aortic app (7) and the THV manufacturer's instructions for use (IFU) for deployment in native aortic valves can recommend a different THV size for the same surgical bioprosthesis size (refer to supplementary materials). At this time, no evidence-based industry sizing or positioning guidelines for

*Wallace H Coulter Department of Biomedical Engineering
Georgia Institute of Technology and Emory University
Technology Enterprise Park, Suite 200
387 Technology Circle, Atlanta, GA 30313
Email address: ajit.yoganathan@bme.gatech.edu (Ajit P. Yoganathan, PhD)

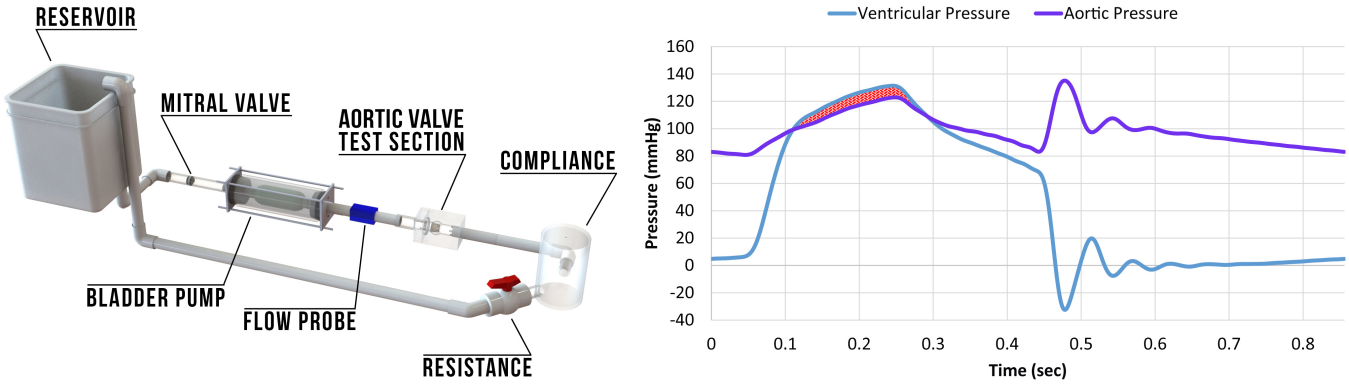

Figure 1: *In Vitro* In Vitro Pulsatile Flow System - The Georgia Tech Left Heart Simulator (left) used in this study is a validated pulsatile flow loop for producing physiologic and pathophysiologic conditions of the heart. The mean TVPG (right) was defined by the average difference between the ventricular and aortic pressure curves as indicated by the shaded region.

VIV-TAVR exist, though it is FDA approved. Furthermore, recent studies suggest that in cases of extreme oversizing of the THV, a supra-annular deployment can result in superior hemodynamics for a balloon-expandable valve in a small bioprosthesis than in the deployment location recommended by the existing guidelines (8, 9, 10). In the current study, we investigate whether or not the drastic effects of supra-annular deployment seen in a small bioprosthesis were still present when there was less prosthesis-patient mismatch. We performed an in vitro study to better understand THV hemodynamics according to valve type, degree of oversizing, and deployment location for balloon- and self-expanding VIV-TAVR.

2. Methods

2.1. Flow Loop

The study was conducted in a validated pulse duplicator (Figure 1) that simulates physiological and pathophysiological conditions of the heart (11). A non-calcified surgical bioprosthesis was mounted into an idealized rigid acrylic chamber designed to simulate the aortic sinus and ascending aorta (Figure 2). The chamber dimensions were based off of published average anatomical measurements (12, 13). The aorto-ventricular angle in the left heart simulator is 0, which is the standard configuration for in vitro TAVR testing for FDA submissions. The flow rate and the aortic and ventricular pressures were tuned to physiological levels through a lumped systemic resistance and compliance and measured through a custom data acquisition system. The working fluid was a 3.5 cSt saline-glycerine solution (approximately 36% glycerine by volume in 0.9% NaCl) to match the kinematic viscosity of blood. Further details of the flow loop are provided in our previous publication (8).

2.2. Valve models and deployment

A 23mm Edwards PERIMOUNT surgical bioprosthesis was implanted in the in vitro model. This surgical bioprosthesis type and size was chosen because it is the among the most commonly encountered in general practice (14, 15). In addition, this surgical valve type and size has multiple recommended THV sizes depending on the guidelines used. For the VIV-TAVR model, THV size selections were based on the recommendations by the VIV app and IFU for deployment in native aortic valves. For the 23mm Edwards PERIMOUNT, both guidelines recommend a 23mm SAPIEN valve, but the VIV app recommends a 23mm CoreValve Evolut and the IFU recommends a 26mm CoreValve. In the current study, a 23mm SAPIEN, a 26mm CoreValve, and a 23mm CoreValve Evolut were deployed within a 23mm Edwards PERIMOUNT surgical bioprosthesis in 5 positions: normal (0mm; bottom of the THV stent aligned with the bottom of the surgical bioprosthesis sewing ring, as indicated by the ViV Aortic app); -3mm and -6mm below the normal position; and +3mm and +6mm above the normal position (Figure 3).

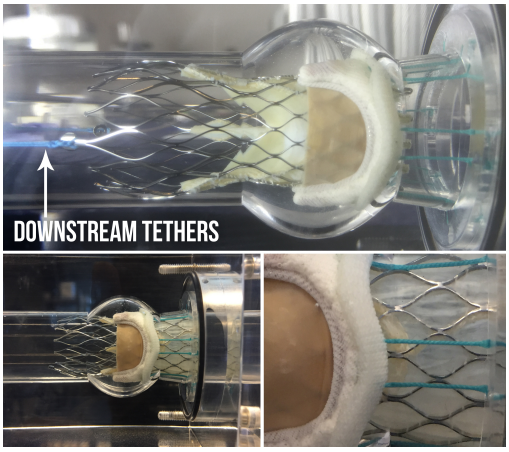

Figure 2: Aortic Chamber - The aortic chamber was designed based on published anatomical average values. Depicted is the 23mm CoreValve Evolut (top) with downstream tethers to resist ventricular migration, within a 23mm PERIMOUNT surgical bioprosthesis. Without tethering, the 23mm CoreValve provided insufficient force to oppose the diastolic gradient and migrated subannularly as a result (bottom).

All valves used in this study were previously unused and non-calcified, and the same THVs were used for all 5 deployment

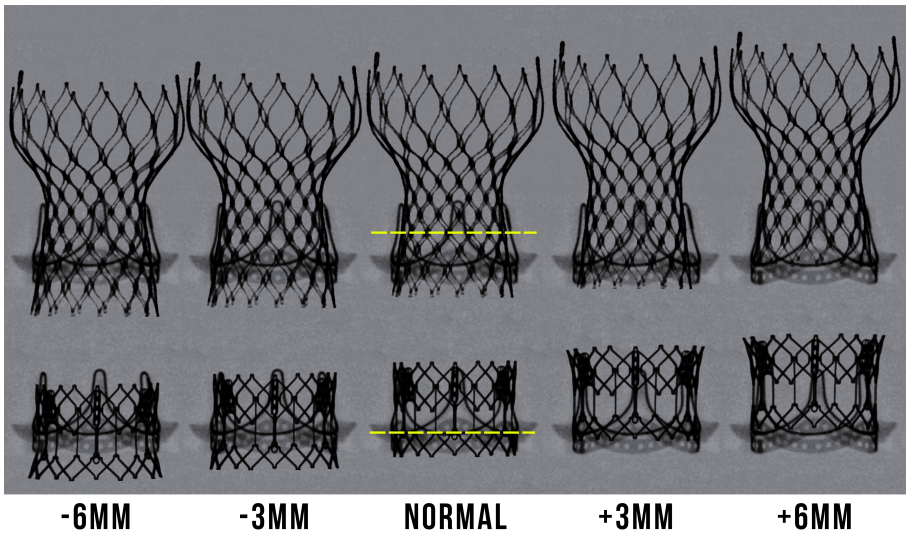

Figure 3: Deployment Schematic - Schematic representation of deployment heights as they would be seen by x-ray. The dashed yellow line indicates the base of the leaflets in the THV. Note the "flower pot" shape taken by the SAPIEN valve in supra-annular deployments.

positions. In order to minimize unnecessary deployments of the balloon-expandable SAPIEN, the valve was never crimped beyond what was required to insert it into the surgical valve (21mm).

Migration was visually assessed by observing the relationship between THV stent struts and the surgical valve stent posts through the optically clear flow chamber before and after flow testing. For the 23mm CoreValve Evolut, the THV migrated to an extreme sub-annular position under physiologic conditions (Figure 2). This was believed to be due to the lack of calcification and decrease distal aorta anchoring force in our model, and thus, the testing of this THV was performed with the valve artificially tethered in the desired deployment location.

2.3. Hemodynamics

VIV performance was characterized using mean transvalvular pressure gradients (TVPG) and regurgitant fraction (RF). The flow loop was tuned to mean arterial pressure of 100 mmHg (Figure 1), a heart rate of 70 bpm, and a cardiac output of 5 L/min with a peak instantaneous systolic flow rate of 25 L/min and a systolic duration of 35%. Two hundred consecutive cardiac cycles (n=200) of hemodynamic data (aortic pressure, ventricular pressure, and flow rate) were collected for each test condition at a 1 kHz data sampling rate using a custom LabVIEW Virtual Instrument.

2.4. Regurgitant Fraction

The level of aortic regurgitation was assessed through comparison of the regurgitant fraction (RF), and was computed from the measured flow waveforms using the following equation:

$$RF = \frac{LV}{SV} \tag{1}$$

where, LV it eh leakage volume and SV is the forward stroke volume. The leakage volume is obtained by subtracting the closing volume from the total regurgitant volume.

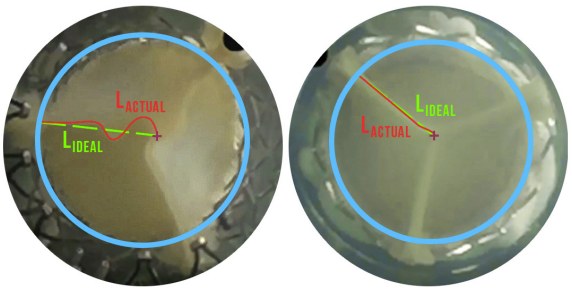

Figure 4: Pinwheeling Index Definition - High-speed en face imaging of the VIV allows for quantification of leaflet deformation. The 26mm CoreValve on the left demonstrates a higher pinwheeling index than the 23mm SAPIEN on the right. Both valves are deployed at the +6mm position.

2.5. Aortic valve orifice area

Effective orifice area (EOA) was computed through the Gorlin equation (16)

$$EOA = \frac{Q}{51.6\sqrt{TVPG}} \tag{2}$$

where, Q is the flow through the aortic valve. This metric is used to evaluate residual stenosis after VIV-TAVR.

2.6. Pinwheeling Index

Based on ISO heart valve guidelines, localized bending of leaflet material, or pinwheeling, should be avoided due to potential for premature tissue degradation (17). This was quantified using en face data by tracing the length of the leaflet free-edges and comparing them to their unconstrained, ideal configurations as described in Figure 4. A pinwheeling index (PI) was computed by following equation:

$$PI = \frac{L_{actual} - L_{ideal}}{L_{ideal}} \tag{3}$$

where, L_{actual} is the length of the leaflet free-edge from the perimeter of the valve to the coaptation center, and L_{ideal} is the straight-line distance between the endpoints of the leaflet free-edge. The value is presented as a percentage.

2.7. Pullout forces

Relative embolization risk for each VIV deployment was evaluated by measuring the pullout force required to dislodge the valve in a different apparatus than the flow studies, and without the downstream tethering. The apparatus and method used to measure pullout force is described to the one used in our previous study (8), however, the downstream region of the CoreValve's stent provides resistance to embolization and necessitated the inclusion of the ascending aorta in our test fixture. The ascending aorta was coated in PTFE matching the coefficient of friction between Nitinol and calcified aortic tissue (approximately 0.15) as reported by previous studies (18, 19, 20). Force was applied gradually until the valve migrated and the peak force measured by a digital force gauge was recorded. Each test condition was repeated 6 times (n=6).

2.8. Statistical analysis

The data are presented as a mean ± standard deviation. Normality of all the data were tested using the Anderson-Darling method. One-way ANOVA was used for analyzing independent sample sets with Tukey's post-hoc test for comparisons between multiple groups. P-values less than 0.05 were considered statistically significant and the analysis was done using SPSS Statistics for Mac (Version 22.0, IBM Corp, NY). A full presentation of the p-values from the post-hoc tests can be found in the supplemental materials.

3. Results

3.1. Hemodynamics

The TVPG is reported as a mean ± standard deviation measured over two hundred consecutive cardiac cycles (n=200) in Figure 5. While we observed that all the measured mean gradients were below the VARC-2 criterion for success of <20 mmHg (21) there were differences between deployment locations according to the valve type. Under the VIV app defined normal deployment positions, the 26mm CoreValve displayed a lower mean gradient than the 23mm CoreValve and 23mm SAPIEN (7.76±0.14 mmHg vs. 10.27±0.18 mmHg vs. 11.66±0.22 mmHg; p<0.01). Both CoreValves performed optimally in the normal to -3mm deployment range, with the mean TVPGs increasing with supra-annular and sub-annular implantation of the THV. On the other hand, the SAPIEN performed better with increasingly supra-annular deployment. The mean TVPG at the 6mm supra-annular deployment is approximately 20% lower than at the normal position (9.31±0.22 mmHg vs 11.66±0.22 mmHg; p<0.01), while a 6mm sub-annular deployment increased gradient by a similar amount.

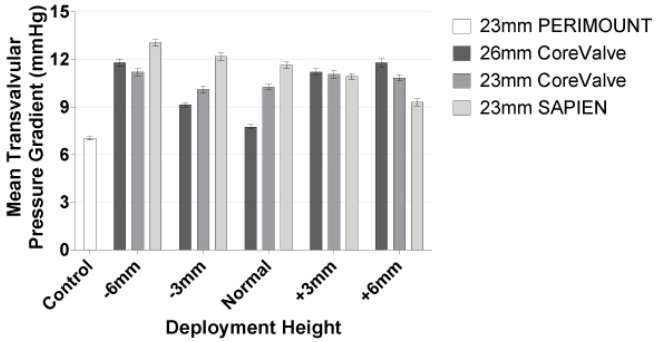

Figure 5: Mean Transvalvular Pressure Gradients - High positioning of the SAPIEN valve lead to more favorable TVPGs, however the deployment recommended by the VIV app yields better gradients for the CoreValves. In addition, the 26mm CoreValve performed better at its optimal deployment than the 23mm CoreValve. The error bars indicate standard deviation and all relevant p-values are less than 0.01, except for comparisons between +3mm deployments for the CoreValves, and between -3mm and normal deployments for the 23mm CoreValve, which were not significantly different.

3.2. Regurgitant Fraction

The RF is reported as a mean ± standard deviation measured over two hundred consecutive cardiac cycles (n=200), and was observed to change with valve type and deployment position as illustrated in Figure 6. Since all deployments demonstrated good coaptation and the closing volume was removed for calculation of RF, the RF value is paravalvular leak (PVL). For the SAPIEN valve, RF progressively decreased as the deployment height increased from -6mm to +6mm (7.40±0.21% to 0.95±0.60%; p<0.01). However, for both CoreValves, sub-annular and supra-annular deployment resulted in higher RF, with the minimum RF observed at the normal deployment position (26mm: 4.79±0.67%; 23mm: 1.98±0.36%; p<0.01). Furthermore, the RF of the 26mm CoreValve was greater than that of the 23mm CoreValve at all deployment positions.

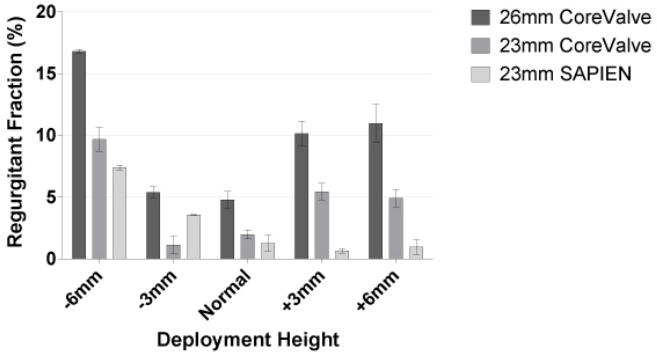

Figure 6: Regurgitant Fraction - The SAPIEN valve had the least regurgitation under normal and supra-annular deployments, whereas the CoreValves performed best in the normal to slightly sub-annular range. The error bars indicate standard deviation and all relevant p-values are less than 0.05.

3.3. Aortic Valve Area

EOA is presented as a mean ± standard deviation measured over two hundred consecutive cardiac cycles (n=200). The vari-

ation of EOA with deployment height for all the THVs mirrored the corresponding changes in mean TVPG (Figure 7). For each THV, the lowest TVPG corresponded to the highest EOA (26 mm CoreValve: 1.66±0.05 cm^2; 23 mm CoreValve: 1.44±0.05 cm^2; 23 mm SAPIEN: 1.51±0.08 cm^2; p<0.01).

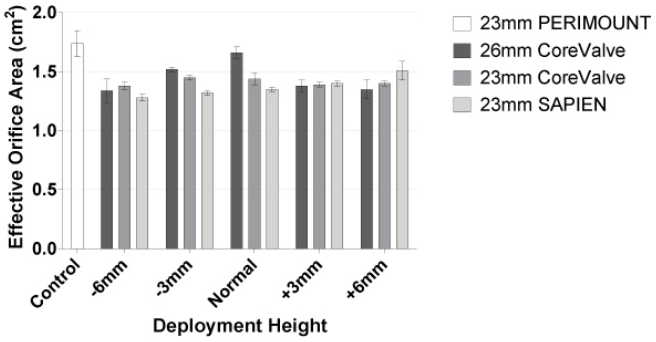

Figure 7: Aortic Valve Area - Supra-annular SAPIEN deployment resulted in increased EOA, whereas normal CoreValve deployment yielded the largest EOA. The 26mm CoreValve performed slightly better than the 23mm CoreValve at its optimal position. The error bars indicate standard deviation and all relevant p-values are less than 0.01, except for comparisons among all +3mm deployment conditions, and between -3mm and normal deployments for the 23mm CoreValve, which were not significantly different.

3.4. Pinwheeling Index

PI values were computed as a means of quantifying the level of excessive leaflet deformation occurring at each deployment, and are presented as a mean standard deviation (n=10) in Figure 8. The SAPIEN had the least amount of pinwheeling when compared to both CoreValve sizes at all the deployment positions (p<0.01). At the normal deployment position, the 26mm CoreValve had significantly larger (approximately 4.5 times) pinwheeling when compared to the 23mm CoreValve (29.13±0.22% vs 6.57±0.14%; p<0.01). Representative extreme pinwheeling cases for each valve can be seen in the supplemental video.

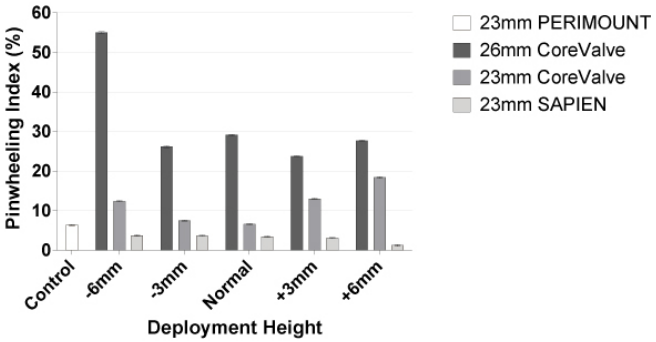

Figure 8: Pinwheeling Index - Pinwheeling index values were computed as a means of quantifying the level of excessive leaflet folding occurring in each deployment. The error bars indicate standard deviation and all relevant p-values were less than 0.01 except for comparisons among -6mm, -3mm, and normal SAPIEN deployments, and between the normal 23mm CoreValve deployment and control which did not show a significant difference.

3.5. Pullout forces

The pullout forces are reported as a mean standard deviation (n=6). The pullout forces were measured only for supra-annular THV deployments because for both the SAPIEN and CoreValves the hemodynamic performance was sub-optimal at sub-annular deployment (Figure 9). In all cases it was observed that the pullout forces decreased with supra-annular deployment. Furthermore at all deployment locations, the pullout force was the highest for the 26mm CoreValve, followed by the 23mm SAPIEN, with the 23mm CoreValve having the lowest pullout forces. None of the THVs experienced antegrade migration under any of the study conditions; however, the 23mm CoreValve Evolut did migrate to an extreme sub-annular position unless it was physically restrained (Figure 2).

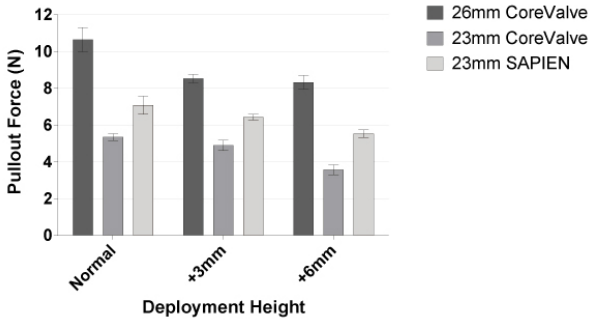

Figure 9: Pullout Forces - The magnitude of force required to dislodge the THV in VIV is shown as measured by a digital force gauge. The error bars indicate standard deviation and all relevant p-values are less than 0.01, except between 3mm and 6mm deployments of the 26mm CoreValve, normal and 3mm deployments of the 23mm CoreValve, and normal and 3mm deployments of the 23mm SAPIEN.

In the case of the SAPIEN, retrograde migration was not a concern because the supra-annular "flower pot" deployment provides additional "geometric" resistance. Systolic hemodynamic forces on the THV were estimated based on the work from Dwyer et al. (22) and are detailed in our previous work (8). A baseline safety threshold was computed to be 0.25 N by Equations 4 and 5.

$$\text{Maximum Systolic Fluid Force} = \frac{TVPG \times A}{0.75} \tag{4}$$

$$A = GOA_{SAVR} - GOA_{TAVR} \tag{5}$$

where GOA_{SAVR} is the maximum surgical bioprosthesis GOA based on the internal diameter of the valve, and GOA_{TAVR} is the geometric orifice area determined via en face imaging of the deployed THV (Figure 4). This is interpreted as the amount of force the fluid imposes on the THV under a peak systolic gradient and represents the theoretical lower limit of pullout force necessary to avoid antegrade embolization. Under a conservative diastolic gradient of 100 mmHg, however, the self-expandable THVs could migrate toward the left ventricle, as was seen with the 23mm CoreValve (Figure 2).

$$\text{Maximum Diastolic Fluid Force} = \frac{MAP \times A_{SAVR}}{0.0133} \approx \frac{MAP \times {D_{SAVR}}^2}{9550} \quad (6)$$

where the mean arterial pressure (MAP) is the diastolic gradient in mmHg, and D_{SAVR} is the true internal diameter of the surgical bioprosthesis in mm. This theoretical maximum diastolic fluid force amounts to 4.62 N, which is in the similar range to that of the 23mm CoreValve deployment pullout force measurements.

4. Discussion

In an in vitro model simulating VIV-TAVR in a 23mm surgical bioprosthesis, we observed that THV hemodynamics met VARC-2 definitions of success (21) for both the SAPIEN and CoreValve THVs. However, hemodynamic performance varied with THV type, size and deployment position. The results of this study (Table 1) suggest that optimal VIV deployment positions exist for both the balloon- and self-expandable THV designs. These optimal positions were determined through an analysis of benefits (mean gradient, valve area) and risks (paravalvular leak, leaflet deformation, and embolization risk). In the case of the SAPIEN, the optimal position is at a supra-annular deployment around 6mm above what is recommended by the ViV Aortic guidance application (7). On the other hand, the optimal deployment for the CoreValve exists at the ViV Aortic application's recommended implantation height. It should be noted that while THVs were developed and tested under current ISO standards, existing recommendations for VIV-TAVR were not developed under such rigorous testing standards. In addition, a deployment that resulted in "device success" in this study is likely to be affected by the characteristics of a stenotic, calcified bioprosthesis in vivo. Thus, these results provide important information on where not to implant THVs, and provide a guide for in vivo evaluation of possible deployment locations.

The improvement in gradients at supra-annular positions for the balloon-expandable valve can be explained by a more complete expansion of the distal portion of the THV, resulting in a "flower pot" deployment. This finding is similar to our previous study, however the effects of supra-annular deployment are not as drastic as the 20 mmHg reduction in mean TVPG seen in a 19mm PERIMOUNT (8). However in the case of the CoreValve, the leaflets are already in a supra-annular position (Figure 3), and thus are less constrained by the bioprosthesis and surrounding anatomy, resulting in optimal gradients at the normal position. Furthermore, the IFU recommended 26mm CoreValve had significantly lower gradients when compared to the ViV Aortic application recommended 23mm CoreValve. This discrepancy highlights the need for hemodynamic performance-based guidelines for VIV-TAVR, as opposed to the ViV Aortic app guidelines, which are strictly based on geometric observations. It also shows that an oversized THV could yield significant improvements in mean post-procedural gradients. As expected, a higher EOA correlated with a lower TVPG for all THVs at all positions.

The occurrence of regurgitation, especially in the form of paravalvular leak, is an important concern for both native valve and VIV-TAVR, since moderate or greater PVL has been associated with worse outcomes after TAVR (23, 24). The lowest leakage was observed at the same positions that resulted in the lowest TVPG, further supporting our recommendation for a supra-annular deployment of the SAPIEN valve, and for a normal deployment of the CoreValve. The 23mm CoreValve valve had substantially lower leakage than the 26mm CoreValve; however, both THVs had less than 5% leakage at the normal deployment position. This difference could be due to incomplete expansion of the over-sized 26mm CoreValve in the semi-rigid bioprosthesis. While THV oversizing results in higher rates of conduction disturbances and annular rupture (25, 26), it has been hypothesized that the "protective effect" of the surgical bioprosthesis ring explains the lower rates of these complications observed with VIV-TAVR (3, 27). Although the leakage for all the valves reported in this study would be classified as mild to mild/moderate regurgitation (21, 28, 29), it should be noted that the in vitro setting represents a conservative scenario. Patient specific anatomical variations and leaflet calcification profiles could result in sub-optimal expansion of the valve leading to higher PVL. Notably, for all valves the highest leakage was observed at the lowest sub-annular position (-6mm), where the sealing of the THV skirt is lower/minimal. Due to aortic stenosis patients' inability to tolerate PVL, it is critical to avoid sub-optimal deployment during VIV-TAVR.

In the case of the CoreValve at sub- and supra-annular positions, the leaflets were observed to deform to a greater extent when compared to the PERIMOUNT. Hence, the pinwheeling index was developed as a novel metric to quantify the severity of this phenomenon. The very mild levels of leaflet deformation exhibited by the control surgical valve were used as a reference for an acceptable PI. The SAPIEN had a lower PI when compared to both CoreValves at all deployment positions. The incomplete expansion of the over-sized CoreValve could result in higher deformation of the THV stent and leaflets leading to higher PI. A counter-intuitive finding of this study was that supra-annular deployment of a 26mm CoreValve resulted in higher gradients, yet little change in the PI than the normal deployment. We speculate that due to the supra-annular leaflet position of the CoreValve, the theoretical benefit of decreased leaflet distortion with a high deployment its lost due to concomitant inlet constriction observed with this deployment location (Figure 10). Higher pinwheeling is associated with increased fatigue loading and accelerated failure of the bioprosthetic leaflets (17). Recent in vitro work on understanding the effect of valve oversizing during TAVR has demonstrated two important results: first, the level of pinwheeling increased with THV oversizing and second, increased pinwheeling was associated with increased leaflet stress levels (30). While THVs are oversized by necessity in order to generate adequate anchoring force, excessively increased stress could lead to decreased

Table 1: Compiled results

	Deployment	Mean TVPG (mmHg) (n = 200)	Regurgitant Fraction (%) (n = 200)	EOA (cm^2) (n = 200)	Pinwheeling Index (%) (n = 10)	Pullout Force (N) (n = 6)
PERIMOUNT	**Control**	7.03 ± 0.10	-	1.74 ± 0.11	6.37 ± 0.13	-
26 mm CoreValve	**-6 mm**	11.80 ± 0.23	16.81 ± 0.17	1.34 ± 0.10	55.02 ± 0.23	-
	-3 mm	9.15 ± 0.14	5.4 ± 0.43	1.52 ± 0.02	26.20 ± 0.23	-
	Normal	**7.76 ± 0.14**	**4.79 ± 0.67**	**1.66 ± 0.05**	29.13 ± 0.22	**10.65 ± 0.66**
	3 mm	11.22 ± 0.21	10.15 ± 1.01	1.38 ± 0.05	**23.76 ± 0.10**	8.53 ± 0.23
	6 mm	11.80 ± 0.25	10.99 ± 1.53	1.35 ± 0.08	27.67 ± 0.16	8.33 ± 0.37
23 mm CoreValve	**-6 mm**	11.20 ± 0.23	9.69 ± 0.96	1.38 ± 0.03	12.39 ± 0.19	-
	-3 mm	**10.11 ± 0.22**	**1.12 ± 0.70**	1.45 ± 0.02	7.50 ± 0.12	-
	Normal	10.27 ± 0.18	1.98 ± 0.36	**1.44 ± 0.05**	**6.57 ± 0.14**	**5.35 ± 0.18**
	3 mm	11.07 ± 0.25	5.44 ± 0.67	1.39 ± 0.02	13.03 ± 0.16	4.90 ± 0.28
	6 mm	10.85 ± 0.20	4.91 ± 0.72	1.40 ± 0.02	18.38 ± 0.23	3.57 ± 0.27
23 mm SAPIEN	**-6 mm**	13.06 ± 0.21	7.40 ± 0.21	1.28 ± 0.03	3.74 ± 0.20	-
	-3 mm	12.20 ± 0.23	3.56 ± 0.05	1.32 ± 0.02	3.67 ± 0.16	-
	Normal	11.66 ± 0.22	1.27 ± 0.66	1.35 ± 0.02	3.46 ± 0.18	**7.09 ± 0.49**
	3 mm	10.94 ± 0.19	**0.66 ± 0.19**	1.40 ± 0.03	3.06 ± 0.14	6.44 ± 0.16
	6 mm	**9.31 ± 0.22**	0.95 ± 0.60	**1.51 ± 0.08**	**1.23 ± 0.22**	5.54 ± 0.20

leaflet durability, and is a very important concern when considering TAVR for the lower-risk patient population. More detailed in vitro and clinical studies are critically needed to determine if such quantitative findings will have a deleterious effect on short-term (<5 years) and/or long-term (10 years) THV durability. As medical imaging advances, such as high speed 4D CT citeMakkar2015b, it may be possible to quantify pinwheeling in vivo.

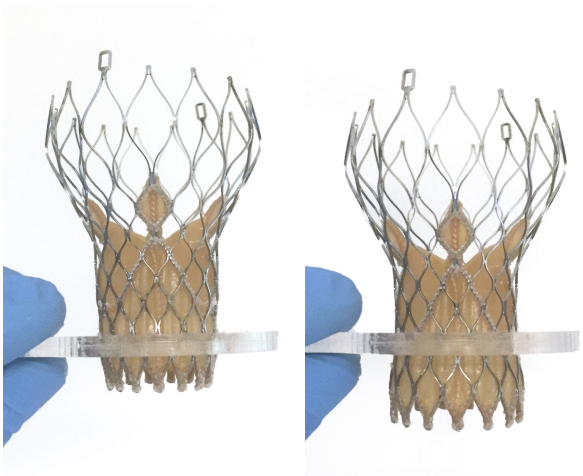

Figure 10: Supra-annular CoreValve Geometric Distortion -A 26mm CoreValve in a 21mm orifice experiences inlet constriction when placed in a supra-annular position (left), when -compared to the normal position (right).

In order to assess the safety of our hemodynamic performance-based deployment recommendations, we evaluated the risk of THV embolization. The highest pullout force was observed at the normal position for all the THVs which is due to the higher contact area between the THV and surgical bioprosthesis, which is consistent with previous work (8). Due to the minimal systolic fluid forces on the THV, antegrade migration does not appear to be a high risk concern. However under a diastolic gradient, the valve which holds the highest risk of retrograde embolization is the 23mm CoreValve, where the pullout force at all positions were very close to the 4.62 N diastolic threshold. While a calcified bioprosthesis may provide additional anchoring for the valve in vivo, this particular VIV combination cannot be recommended by this in vitro study due to observed retrograde migration (Figure 2) in a non-calcified bioprosthesis. This finding underscores the need to weigh the risks and benefits when using this valve combination in vivo.

5. Conclusions

We performed a controlled parametric in vitro study of VIV-TAVR in a 23mm PERIMOUNT. Based on an analysis of benefits (mean gradient, valve area) versus risks (paravalvular leak, leaflet deformation, and embolization), the optimal deployment for the 23mm SAPIEN valve is at +6mm supra-annular position, and at the normal position for both the 23mm and 26mm CoreValves. Furthermore, the 26mm CoreValve had better hemodynamic performance than the 23mm CoreValve at the normal position, but at the risk of higher PI and potentially reduced leaflet durability. It is reassuring that all VIV-TAVR deployments were consistent with the definitions of VARC-2 procedural success (21). We acknowledge that extreme supra-annular deployment may not always be possible based on anatomical and procedural constraints, and that it may be risky for operators with limited TAVR experience. In addition, newer THV and surgical valve design features may pose additional challenges to be overcome in the pursuit of an optimal VIV deployment. For instance, it is unknown what affect the SAPIEN 3 skirt may have on forces resisting migration, as well as inflow resistance in a high implantation VIV scenario. While

this study has demonstrated the robustness of these THVs, it underscores the need for rigorous performance- and safety-based recommendations. The clinical, industrial, and regulatory communities need to be aware that such risk/benefit analyses are critical going forward for the use of THVs in VIV applications, especially in the lower risk patient population.

6. Acknowledgments

The authors would like to acknowledge the members of the Cardiovascular Fluid Mechanics Laboratory for their assistance and feedback. The work at the Cardiovascular Fluid Mechanics Laboratory at the Georgia Institute of Technology was funded through discretionary funds available to the Principal Investigator, such as the Wallace H Coulter Endowed Chair.

References

[1] Kishore J Harjai, Jean-Michel Paradis, and Susheel Kodali. Transcatheter aortic valve replacement: game-changing innovation for patients with aortic stenosis. *Annual review of medicine*, 65:367–83, jan 2014.

[2] Danny Dvir, John G Webb, Sabine Bleiziffer, Miralem Pasic, Ron Waksman, Susheel Kodali, Marco Barbanti, Azeem Latib, Ulrich Schaefer, Josep Rodés-Cabau, Hendrik Treede, Nicolo Piazza, David Hildick-Smith, Dominique Himbert, Thomas Walther, Christian Hengstenberg, Henrik Nissen, Raffi Bekeredjian, Patrizia Presbitero, Enrico Ferrari, Amit Segev, Arend de Weger, Stephan Windecker, Neil E Moat, Massimo Napodano, Manuel Wilbring, Alfredo G Cerillo, Stephen Brecker, Didier Tchetche, Thierry Lefèvre, Federico De Marco, Claudia Fiorina, Anna Sonia Petronio, Rui C Teles, Luca Testa, Jean-Claude Laborde, Martin B Leon, and Ran Kornowski. Transcatheter Aortic Valve Implantation in Failed Bioprosthetic Surgical Valves. *JAMA*, 312(2):162, jul 2014.

[3] Danny Dvir, Marco Barbanti, John Tan, and John G Webb. Transcatheter aortic valve-in-valve implantation for patients with degenerative surgical bioprosthetic valves. *Current problems in cardiology*, 39(1):7–27, jan 2014.

[4] Nicolaj Hansson, Tina Leetmaa, Jonathon A. Leipsic, Kaare Jensen, Henning Rud Andersen, Jesper M. Jensen, John Webb, Philipp Blanke, Marianne Tang, and Bjarne Nørgaard. TCT-665 Early Aortic Transcatheter Heart Valve Thrombosis: Diagnostic Value of Contrast-Enhanced Multislice Computed Tomography. *Journal of the American College of Cardiology*, 64(11):B193–B194, sep 2014.

[5] Eduardo De Marchena, Julian Mesa, Sydney Pomenti, Christian Marin y Kall, Ximena Marincic, Kazuyuki Yahagi, Elena Ladich, Robert Kutz, Yaar Aga, Michael Ragosta, Atul Chawla, Michael E. Ring, and Renu Virmani. Thrombus Formation Following Transcatheter Aortic Valve Replacement. *Journal of the American College of Cardiology: Cardiovascular Interventions*, 8(5):728–739, 2015.

[6] Raj R. Makkar, Gregory Fontana, Hasan Jilaihawi, Tarun Chakravarty, Klaus F. Kofoed, Ole de Backer, Federico M. Asch, Carlos E. Ruiz, Niels T. Olsen, Alfredo Trento, John Friedman, Daniel Berman, Wen Cheng, Mohammad Kashif, Vladimir Jelnin, Chad a. Kliger, Hongfei Guo, Augusto D. Pichard, Neil J. Weissman, Samir Kapadia, Eric Manasse, Deepak L. Bhatt, Martin B. Leon, and Lars Søndergaard. Possible Subclinical Leaflet Thrombosis in Bioprosthetic Aortic Valves. *New England Journal of Medicine*, page 151005110046004, 2015.

[7] Vinayak Bapat. Valve in Valve Aortic App version 2.0, 2015.

[8] Prem A. Midha, Vrishank Raghav, Jose F. Condado, Sivakkumar Arjunon, Domingo E. Uceda, Stamatios Lerakis, Vinod H. Thourani, Vasilis Babaliaros, and Ajit P. Yoganathan. How Can We Help a Patient With a Small Failing Bioprosthesis? *JACC: Cardiovascular Interventions*, 8(15):2026–2033, dec 2015.

[9] Danny Dvir. Treatment of Small Surgical Valves. *JACC: Cardiovascular Interventions*, pages 1–3, 2015.

[10] Ali N Azadani, Nicolas Jaussaud, Peter B Matthews, Liang Ge, T Sloane Guy, Timothy A M Chuter, and Elaine E Tseng. Valve-in-valve implantation using a novel supravalvular transcatheter aortic valve: proof of concept. *The Annals of thoracic surgery*, 88(6):1864–9, dec 2009.

[11] Choon Hwai Yap, Neelakantan Saikrishnan, Gowthami Tamilselvan, and Ajit P. Yoganathan. Experimental measurement of dynamic fluid shear stress on the aortic surface of the aortic valve leaflet. *Biomechanics and Modeling in Mechanobiology*, 11(1-2):171–182, jan 2012.

[12] Joseph Knight, Vartan Kurtcuoglu, Karl Muffly, William Marshall, Paul Stolzmann, Lotus Desbiolles, Burkhardt Seifert, Dimos Poulikakos, and Hatem Alkadhi. Ex vivo and in vivo coronary ostial locations in humans. *Surgical and radiologic anatomy : SRA*, 31(8):597–604, oct 2009.

[13] H. Reul, A. Vahlbruch, M. Giersiepen, Th. Schmitz-Rode, V. Hirtz, and S. Effert. The geometry of the aortic root in health, at valve disease and after valve replacement. *Journal of Biomechanics*, 23(2):181–191, jan 1990.

[14] Douglas R. Johnston, Edward G. Soltesz, Nakul Vakil, Jeevanantham Rajeswaran, Eric E. Roselli, Joseph F. Sabik, Nicholas G. Smedira, Lars G. Svensson, Bruce W. Lytle, and Eugene H. Blackstone. Long-Term Durability of Bioprosthetic Aortic Valves: Implications From 12,569 Implants. *The Annals of Thoracic Surgery*, 99(4):1239–1247, apr 2015.

[15] Danny Dvir and John G. Webb. Transcatheter Aortic Valve-in-Valve Implantation for Patients With Degenerative Surgical Bioprosthetic Valves. *Circulation Journal*, 79(4):695–703, jan 2015.

[16] Neelakantan Saikrishnan, Gautam Kumar, Fadi J Sawaya, Stamatios Lerakis, and Ajit P Yoganathan. Accurate assessment of aortic stenosis: a review of diagnostic modalities and hemodynamics. *Circulation*, 129(2):244–53, jan 2014.

[17] International Standards Organization. ISO 5840-3: 2013, Cardiovascular implants Cardiac valve prostheses Part 3: Heart valve substitutes implanted by transcatheter techniques. Technical report, Geneva, Switzerland, 2013.

[18] Joseph Mummert, Eric Sirois, and Wei Sun. Quantification of biomechanical interaction of transcatheter aortic valve stent deployed in porcine and ovine hearts. *Annals of biomedical engineering*, 41(3):577–86, mar 2013.

[19] Siddharth Vad, Amanda Eskinazi, Timothy Corbett, Tim McGloughlin, and Jonathan P Vande Geest. Determination of Coefficient of Friction for Self-Expanding Stent-Grafts. *Journal of Biomechanical Engineering*, 132(12):121007, 2010.

[20] Shijia Zhao, Linxia Gu, and Stacey R. Froemming. Finite Element Analysis of the Implantation of a Self-Expanding Stent: Impact of Lesion Calcification. *Journal of Medical Devices*, 6(2):021001, 2012.

[21] Arie Pieter Kappetein, Stuart J Head, Philippe Généreux, Nicolas M van Mieghem, Eugene H Blackstone, Thomas G Brott, David J Cohen, Donald E Cutlip, Gerrit-Anne van Es, Rebecca T Hahn, Ajay J Kirtane, Mitchell W Krucoff, Susheel Kodali, Michael J Mack, Roxana Mehran, Josep Rodés-Cabau, Pascal Vranckx, John G Webb, Stephan Windecker, Patrick W Serruys, and Martin B Leon. Updated standardized endpoint definitions for transcatheter aortic valve implantation: the Valve Academic Research Consortium-2 consensus document. *Journal of the American College of Cardiology*, 60(15):1438–54, oct 2012.

[22] Harry A Dwyer, Peter B Matthews, Ali Azadani, Liang Ge, T Sloane Guy, and Elaine E Tseng. Migration forces of transcatheter aortic valves in patients with noncalcific aortic insufficiency. *The Journal of thoracic and cardiovascular surgery*, 138(5):1227–33, nov 2009.

[23] Susheel K Kodali, Mathew R Williams, Craig R Smith, Lars G Svensson, John G Webb, Raj R Makkar, Gregory P Fontana, Todd M Dewey, Vinod H Thourani, Augusto D Pichard, Michael Fischbein, Wilson Y Szeto, Scott Lim, Kevin L Greason, Paul S Teirstein, S Chris Malaisrie, Pamela S Douglas, Rebecca T Hahn, Brian Whisenant, Alan Zajarias, Duolao Wang, Jodi J Akin, William N Anderson, and Martin B Leon. Two-Year Outcomes after Transcatheter or Surgical Aortic-Valve Replacement. *New England Journal of Medicine*, 366(18):1686–1695, may 2012.

[24] Corrado Tamburino, Davide Capodanno, Angelo Ramondo, Anna Sonia Petronio, Federica Ettori, Gennaro Santoro, Silvio Klugmann, Francesco Bedogni, Francesco Maisano, Antonio Marzocchi, Arnaldo Poli, David Antoniucci, Massimo Napodano, Marco De Carlo, Claudia Fiorina, and Gian Paolo Ussia. Incidence and Predictors of Early and Late Mortality After Transcatheter Aortic Valve Implantation in 663 Patients With Severe Aortic Stenosis. *Circulation*, 123(3):299–308, jan 2011.

[25] Ronald K. Binder, John G. Webb, Stefan Toggweiler, Melanie Freeman, Marco Barbanti, Alexander B. Willson, Donya Alhassan, Cameron J. Hague, David A. Wood, and Jonathon Leipsic. Impact of Post-Implant SAPIEN XT Geometry and Position on Conduction Disturbances, Hemodynamic Performance, and Paravalvular Regurgitation. *JACC: Cardiovascular Interventions*, 6(5):462–468, may 2013.

[26] Philipp Blanke, J. Reinohl, Christian Schlensak, Matthias Siepe, Gregor Pache, Wulf Euringer, Annette Geibel-Zehender, Christopher Bode, Mathias Langer, Friedhelm Beyersdorf, and Manfred Zehender. Prosthesis Oversizing in Balloon-Expandable Transcatheter Aortic Valve Implantation Is Associated With Contained Rupture of the Aortic Root. *Circulation: Cardiovascular Interventions*, 5(4):540–548, aug 2012.

[27] Vinayak Bapat, Izanne Mydin, Sucharitha Chadalavada, Hassan Tehrani, Rizwan Attia, and Martyn Thomas. A guide to fluoroscopic identification and design of bioprosthetic valves: A reference for valve-in-valve procedure. *Catheterization and Cardiovascular Interventions*, 81(5):853–861, apr 2013.

[28] Rick A Nishimura, Catherine M Otto, Robert O Bonow, Carlos E Ruiz, Paul Sorajja, Blase A Carabello, John P Erwin, Robert A Guyton, Patrick T O'Gara, Carlos E Ruiz, Nikolaos J Skubas, Paul Sorajja, Thoralf M Sundt, James D Thomas, Jeffrey L Anderson, Jonathan L Halperin, Nancy M Albert, Biykem Bozkurt, Ralph G Brindis, Mark A Creager, Lesley H Curtis, David DeMets, Judith S Hochman, Richard J Kovacs, E Magnus Ohman, Susan J Pressler, Frank W Sellke, Win-Kuang Shen, William G Stevenson, and Clyde W Yancy. 2014 AHA/ACC guideline for the management of patients with valvular heart disease: a report of the American College of Cardiology/American Heart Association Task Force on Practice Guidelines. *Journal of the American College of Cardiology*, 148(22):e1–e132, jun 2014.

[29] Stamatios Lerakis, Salim S. Hayek, and Pamela S. Douglas. Paravalvular Aortic Leak After Transcatheter Aortic Valve Replacement: Current Knowledge. *Circulation*, 127(3):397–407, jan 2013.

[30] Hoda Maleki, Shahrokh Shahriari, Michel Labrosse, Josep Rodés-Cabau, Philippe Pibarot, and Lyes Kadem. Effect of Aortic Annulus Size and Prosthesis Oversizing on the Hemodynamics and Leaflet Bending Stress of Transcatheter Valves: An In Vitro Study. *Canadian Journal of Cardiology*, 31(8):1041–1046, aug 2015.